IRAQI Academic Scientific Journals

Samarra Journal of Pure and Applied Science

SJPAS

www.sjpas.com

p ISSN: 2663-7405
e ISSN: 2789-6838

Antagonism between carbon nano particles adsorption and virulence of pseudomonas aeruginosa

Sarah Adnan Khalaf *, Sufyan mohammed shartooh, Mayada Abdullah shehan
Department of Biolgy, College of Science, University of Anbar, Al-Anbar, Ramadi. Iraq.

https://doi.org/10.54153/sjpas.2026.v8i1.1128

Article Information

Received: 11/01/2025
Revised: 15/02/2025
Accepted: 20/02/2025
Published: 30/12/2025

Keywords:

pseudomonas aeruginosa, biosorption, carbon nano particles, TEM, SEM, XRD

Corresponding Author

E-mail:
sar22s1001@uoanbar.edu.iq

Abstract

The aqueous environment contamination by pseudomonas has become a great challenge for human beings. Walnut shells were washed by distilled water, mixed with KOH, burned at 650°C, and treated ultrasonically to obtain carbon nanoparticles. The bacterial isolates were from different sites of domestic water in hospitals and characteristic the *pseudomonas*. After that the minimum inhibitory concentration (MIC) was done to determine the optimum concentration that affected on *p.aeruginosa* and it was 0.006 mg/l , then using of polymerase chain reaction (PCR) to detect virulence factor genes (copB *and czcA*) and they characterized by biochemical and morphological diagnosis of *p.aeruginosa* in five isolates. Following treatment, the copB gene expression was 0.211 for isolate 2 and 0.047 for isolate 3, while the czcA gene expression was 0.882 for isolate 10 and 0.392 for isolate 11. The capacity of CNPs to reduce the gene expression in virulence factor genes was tested by using quantitative PCR (qPCR), as a result that affects bacteria, the CNPs at certain concentrations has high capacity to identify the virulence factors genes. These results were supported by XRD examination (Panalytical 'X' Pert Pr, UK), which indicated the presence of two Bragg diffraction peaks in the carbon nanoparticles, TEM (Zeiss LEO 912 AB/ Germany) results also showed the presence of inhomogeneous particles, as well as the irregular shape of the surface of the carbon nanoparticles with a large surface area, according to SEM examination (Zeiss Sigma VP/ Germany).

Introduction

One of the main risks to the aquatic environment globally is thought to be microorganism-induced water pollution. Hospitals, industry, animal farms, and fecal waste all contribute to the bacterial load in a body of water. For a long time, the notion of public health security has been based on the employment of coliform groups of bacteria as an indicator organism for microbial contamination of water [1].

The genus Pseudomonas aeruginosa is one of the most diverse and ecologically significant groups of bacteria on the planet, partly because of its long evolutionary history. It is a

pathogenic bacterial species that causes infections and diseases, including several illnesses in humans, especially in patients with compromised immune systems, and numerous infections acquired in hospitals. *Pseudomonas* species are thought to have a significant habitat in drinking water [2]. Among the genus's notable traits are its prototrophic nature, metabolic adaptability, genome flexibility, and capacity to withstand many types of stress (including those caused by chemicals, physical agents, and antibacterial substances).

Growth of pseudomonas is also expected to be possible in the final drinking water. In hospital settings, this bacterium is a highly significant pathogen, accounting for nearly 10% of nosocomial infections. When resistance mechanisms against the majority of standard antibiotics develop, it leads to infections that are difficult to cure [3].

The virulence factors required for an infection to proliferate and spread illness First, lipopolysaccharide (LPS), an essential surface structural element, protects the lipid and the outer leaflet. Tissue damage, adhesion, and host receptor recognition are all made possible by endotoxicity in LPS [4]. There may be a link between LPS and the formation of biofilms and antibiotic tolerance. Second, outer membrane proteins (OMPs) enhance adhesion, food exchange, and antibiotic resistance. Additionally, drug resistance resulting from biofilm development is associated with the flagellum, pili, and other adhesins. Fourth, there are six distinct types of secretion systems, including flagella (which are associated with T6SS). In reaction to chemotactic signals, pili (T4SS) and the multi-toxin components type 3 secretion system (T3SS) are responsible for adhesion, swimming, swarming, and colonization of hosts. Finally, it is possible that exopolysaccharides such as Pel, PSL, and alginate would encourage the development of biofilms while inhibiting the elimination of microbes [5].

Moreover, it has been shown that the size and surface area of carbon nanomaterials are two important variables affecting their antibacterial activity. In other words, reducing the size of the nanoparticles and increasing their surface area improves their ability to interact with bacteria [6]. It has been suggested that oxidative stress caused by carbon-based nanomaterials damages bacterial membranes.

The ability of nanoparticles (NPs) to suppress bacterial illnesses is quite strong. To attain encouraging bactericidal efficacy [7]. This paper focuses on the role of carbon nanoparticles to reduce the diffusion of bacteria and its virulence factors genes.

Materials and Methods

Preparation of carbon nanoparticles: walnut peel was mixed with KOH in a ratio of 1:1.5 (w/w). Then heated at 650 °C for two hours. After a neutral pH was achieved, the produced material (carbon) was cleaned with distilled water to get rid of any remaining KOH, metallic materials, and impurities. It was then dried in an oven at 50 °C for six hours and ultrasonically treated at 20 kh for one hour (figure 1) [8].

A B

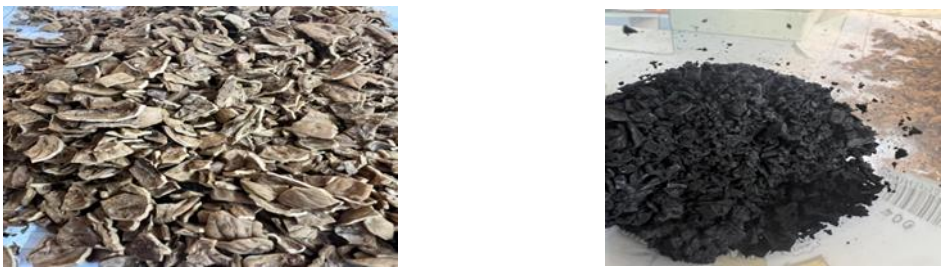

Fig. 1 *Walnut peel (A)mixed with KOH to prepare carbon nano particles(B)*

X Ray Diffraction (XRD)

This method is based on the principle that materials will both scatter and absorb radiation. Materials can be identified using the scattered radiation by analyzing their crystalline or organized structure's diffraction pattern [9].

Transmission electron microscopy (TEM)

This approach is based on applying electrons to a specimen that is spread out on a carbon sheet that looks like lace. When the incident electron beam passes through the sample, it will undergo a variety of changes, including interactions with sample atoms that cause elastic, inelastic, and unscattered electrons. When electrons leave a specimen, they will carry information about its structure [10].

Scanning electron microscopy (SEM)

When examining the morphology of materials, the scanning electron microscope (SEM) is a crucial tool. Its main strategy is to accelerate the incoming electron beam as it approaches a sample. Numerous signals are produced as a result of the interaction between the sample and the electron beam. They are mostly backscattered electrons (BSE), distinctive X-rays, and secondary electrons [11].

Isolation of *p.aeruginosa*

Fifteen water samples were collected from 15 hospitals water of al-anbar governorate), the samples were inoculated on blood agar and aerobically incubated for 24 hours at 42 °C. In order to identify the colonies as P. aeruginosa, further biochemical tests, oxidase-positive, urease-negative, colony morphology, and growth at 42 °C were employed [12]. Biochemical assays and the odor of specific media in cultures were used to identify Pseudomonas aeruginosa isolates.

Determination of minimum inhibitory concentration

A serial of dilutions in test tubes was used to determine the carbon nanoparticle solution's minimum inhibitor concentration (MIC) (5 tubes for each isolate). each tube contained 9 ml of normal saline, then 100 µl of test material (0,06 g carbon nanoparticles). Pipetting from the first tube that incubated 24 hours of nanocarbon with bacterial culture to the next tube, then cultured on medium and incubated for 24 hours resulted in serial dilution.

Molecular methods

Extraction of genomic DNA

After adding bacterial culture, 5 milliliters of brain heart infusion broth were heated for incubation. Before creating each broth, the bacterial cells were spun for two minutes at 14500

rpm in a 1.5 ml Eppendrof tube. The bacterial cells were centrifuged for two minutes at 14500 rpm in a 1.5 ml Eppendrof tube as the first step in making each broth. The particle was kept in a deep freezer at -20 degrees Celsius for later use, while the supernatant was thrown away. The bacterial isolates' genomic DNA was extracted and purified using a microbiome DNA isolation kit (Norgen-Canada).

Genomic DNA band detection using 1% agarose gel electrophoresis

Bands of genomic DNA were identified using the agarose gel electrophoresis technique. 1% agarose gel. When the agarose gel was ready, 5 µl of the ladder (100 pb) was added to the gel's first well. then the PCR products (5 µl) were added to the agarose gel wells, and the electric current was matched for one and a half hours at 70 volts. The DNA bands were then found at 350 nm using an ultraviolet light after the gel had been placed under a UV transilluminator. In the end, pictures of the discernible stripes were taken [13].

Carbon nano particles resistance genes pcr screening

A list of the PCR primers used for this study is provided below [14] . contributed their knowledge to the development of Pseudomonas aeruginosa-specific primers for copB and czcA. Table 1, shows the measurements for each delivery. 30 cycles of one minute each at 94 °C make up the PCR cycle, which is followed by another 4 minutes at 94 °C. For one more minute, the temperature falls to 57 °C, and then it increases to 72 °C. At 72 degrees Celsius, the final extension takes eight minutes. In this study, two PCR tests were utilized.

Table 1: Primers, sequences and sizes

Gene	Sequence (5' - 3')	Product size (bp)	References
CopB	F:GGTTGGTCAACAGGATGTCGTACT R:TTCCTGCTCGACCAGTTGGAATAC	364	(Muslim & Al-Saadi, 2023)
CzcA	F:ACAGGTTGCGGATGAAGGAGATCA R:GTTCACCTTGCTCTTCGCCATGTT	206	(Muslim & Al-Saadi, 2023)

RNA isolation method

Precipitate the RNA

a. Add five to ten micrograms of RNase-free glycogen to the aqueous phase in order to transfer tiny initial samples (less than 106 cells or 10 mg of tissue).

Note: Although the glycogen and RNA co-precipitate, this does not affect later uses.

b. After adding 1 mL of TRIzol™ to the aqueous phase, lyse it with 0.5 mL of isopropanol.

c. Incubate for 10 minutes.

d. For ten minutes, centrifuge at 12,000 × g and 4°C. A white, gel-like pellet made of the whole RNA precipitate appears at the tube's bottom.

e. The supernatant should be discarded using a micropipette.

Wash the RNA

a. By combining 1 milliliter of 75% ethanol with 1 milliliter of the TRIzolTM Reagent for lysis, the pellet can be recovered. The RNA might be kept in 75% ethanol, for instance, for a year at -20°C or for a week at 4°C.

b. After vortexing, centrifuge the sample at 7500 × g for 5 minutes at 4°C

c. Discard the supernatant using a micropipette

d.Dry the RNA pellet for 5-10 minutes under a vacuum or by air.

Solubilize the RNA

a. For re-suspension, press the pellet up and down in 20–50 µL of RNase-free water, 0.1 mM EDTA, or 0.5% SDS solution.

b. Put it in a water bath or heat block that is set to between fifty and sixty degrees Celsius for ten to fifteen minutes. It may be kept at -70°C or used again.

Luna Universal qPCR Master Mix Protocols

The fluorescence of a double-stranded DNA (dsDNA) binding dye, most commonly SYBR® Green I, is used in dye-based quantitative PCR (qPCR), which measures DNA amplification in real time throughout each PCR cycle. When it is possible to consistently differentiate the fluorescence signal from the background fluorescence,

Component	20 µl Reaction	Final concentration
Master Mix for Luna Universal qPCR	10 µl	1 X
Forward primer(10µM)	0.5 µl	0.25
Reverse primer(10µM)	0.5 µl	0.25
Template DNA	Variable	100 ng<
Nuclease free water	To 20 µl	

1. All reaction ingredients, including the Luna Universal Probe qPCR Master Mix, should be frozen with ice at room temperature. To quickly combine the ingredients once they have all thawed, use pipetting, mild vortexing, or inversion.

2. Use a pipette or vortex to mix gently yet thoroughly. Use a quick centrifugation to gather the liquid at the tube's bottom.

3. The test mixture should be aliquoted onto a qPCR tube or plate. For best results, minimize bubbles and utilize exact, constant pipetting volumes.

4. To qPCR tubes or plates, add DNA templates. Use optically transparent film for plates and flat, transparent covers for tubes. Properly sealing plate corners and edges is crucial to avoiding artifacts caused by evaporation.

5. To eliminate bubbles and gather liquid, spin tubes or plates for a brief period of time (one minute at 2,500–3,000 rpm). 6. Use the specified thermocycling methodology to program the real-time instrument (see table below). Make sure the extension step concludes with a plate read. Utilize the real-time instrument's SYBR or SYBR/FAM scan mode preset.

Result and discussion
Carbon nanoparticles
X-Ray Diffraction (XRD)

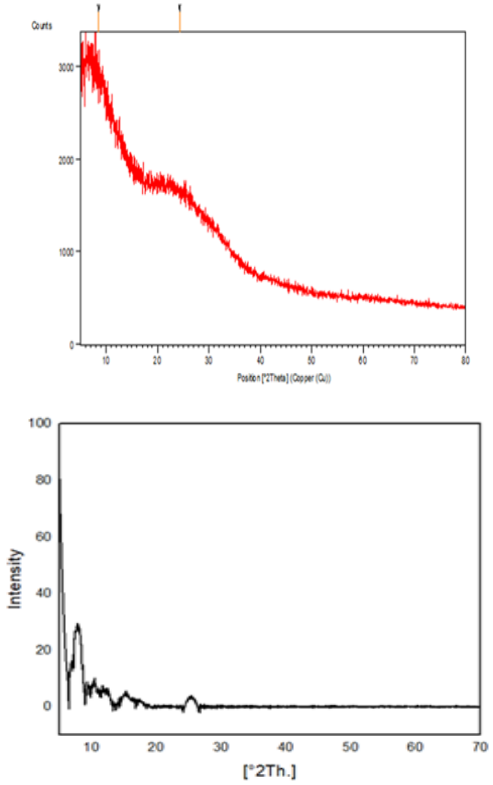

Fig. 2 *XRD of carbon nanoparticles*

Carbon nanoparticles' structural structure was ascertained by X-ray powder diffractometric analysis. The XRD spectrum of the carbon nanoparticles shows two Bragg diffraction peaks at around 2θ = 8.9o and 16.01 in Figure 2. the XRD peak at 2θ = 8.o, indexed as (002), indicates the existence of substantial amounts of amorphous material in respect to multi-walled carbon nanotubes. Low-quality carbon nanomaterials are indicated by the peak around 2θ = 14.5o, which is indexed as the (101) plane. the peak around 2θ = 23.4, which is indexed as the (101) plane, indicates the presence of hexagonal graphite lattice. The current investigation's peaks at 2θ = 17 were classified as (002) planes, suggesting the presence of substantial amounts of amorphous carbon nanomaterials and a hexagonal graphite lattice [15].

Scanning electron microscopy (FE-SEM):

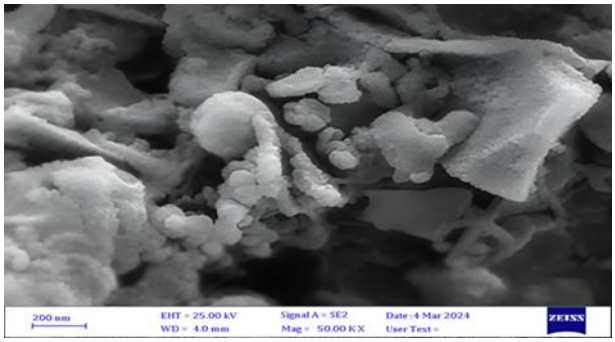

Fig. 3 *FESEM of carbon nanoparticles*

SEM was utilized to track how the changes made to the carbon nanoparticle production process affected the surface morphology. The carbon is comprised of irregularly shaped particles with rough surfaces and caves, as shown by the FE-SEM images in Fig 3. This

suggests a high specific surface area. This is because the walnut shell chains are destroyed when they are burned via a tiny hole at a temperature above 600¯ after being mixed with potassium hydroxide (KOH)[16].

Transmission electron microscopy (TEM)

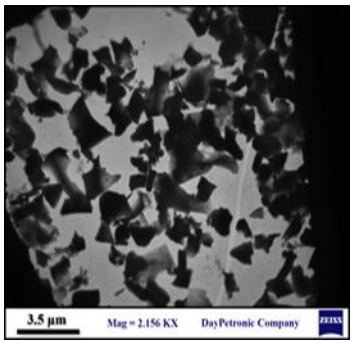

Fig. 4 *TEM of carbon nano paticles*

TEM pictures of carbon nanoparticles made using method 2.2 show that the nanoparticles were generating particles smaller than 3.5 nm in diameter. The existence of inhomogeneous particles was detected by TEM analysis (Figure 4), which may have resulted from the inner zone's inadequate temperature. The size of the CNPs generated differed throughout samples, suggesting that the temperature during heating could be the main determinant of the CNPs' sizes [17].

Isolation of *p.aeroginosa*

The big, flat, dark greenish colonies from blood agar were analyzed following subculturing on nutrition agar. All of the other P. aeruginosa microscopic diagnostic, culturing, and biochemical identification test findings are shown in table 2:

Table 2: The results of *Pseudomonas* diagnosis b different test

Phenotypic and biochemical tests	P. aeruginosa result
Oxidase Test	+
Gram Staining	-
Grow on Cetrimide Agar	+
Catalase Test	+
Grow in 42 Oc	+
Shape	Rod
Urease test	-

+ indicated positive result, - indicates negative result

The MIC and synergistic effect of CNPs solutions

Table 3: numbers of colonies after treatment with CNPs

No	Con 0.001µg/l	Con 0.002 µg/l	Con 0.003µg/l	Con 0.004µg/l	Con 0.005µg/l	Con 0.006 µg/l
1	250	230	200	200	80	0
2	240	150	80	70	40	20
3	90	70	50	40	30	10
4	220	200	190	80	10	0
5	-	-	-	-	-	-
6	270	260	220	200	100	50
7	-	-	-	-	-	-
8	-	-	-	-	-	-
9	190	110	95	73	52	30
10	140	115	70	60	30	8
11	115	97	80	65	20	5
12	-	-	-	-	-	-
13	-	-	-	-	-	-
14	-	-	-	-	-	-
15	-	-	-	-	-	-

Presence of metal Resistance Genes

Pseudomonas aeruginosa isolates were molecularly identified using specific PCR primers for the *copB* and *czcA* genes. These genes are present in the pan-resistance operon of the sequenced isolates of Pseudomonas aeruginosa (Figures 5 and 6). Amplification of *czcA* was positive in all five environmental samples (33%). Heavy transport is accomplished by the efflux pump *czcA,* a reverse divalent cation-proton transporter [18] Of them, five (33%) had *copB*.To make the battery resistant to copper, *CopB* are sufficient [19] [20]. The results of MIC showed the diversity of respond to CNPs by *p.aeruginosa* (figure 7).

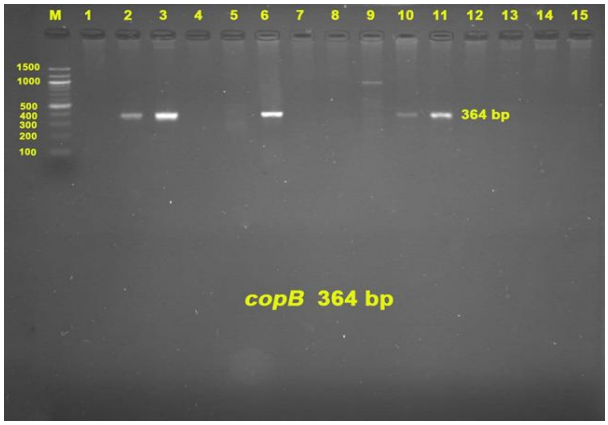

Fig. 5 *PCR products (364 bp) generated using copB-specific primers were electrophoresed on an agarose gel; positive findings were detected in lanes 2, 3, 6, 10, and 11, with lane M representing a DNA ladder.*

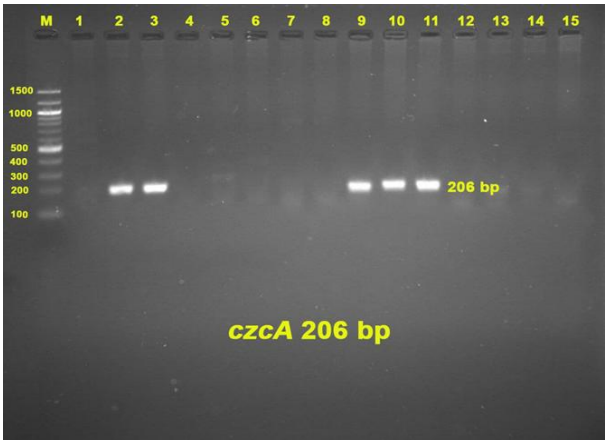

Fig. 6 *PCR products (206 bp) generated using czcA-specific primers were electrophoresed on an agarose gel; positive findings were detected in lanes 2, 3, 9, 10, and 11, with lane M representing a DNA ladder.*

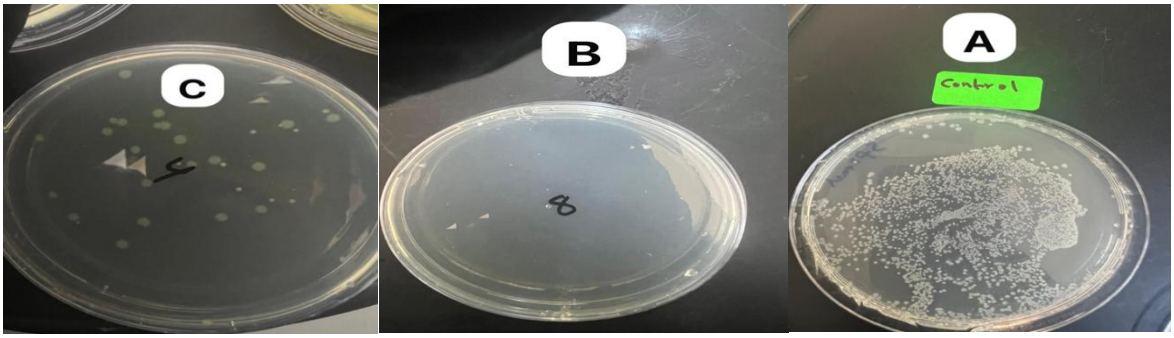

Fig. 7 ***(A)*** *bacterial isolate growth on culture media before incubation with CNPs* ***(B) (C)*** *bacterial isolates after treatment with CNPs.*

Gene expression and real time PCR of copB and czcA genes

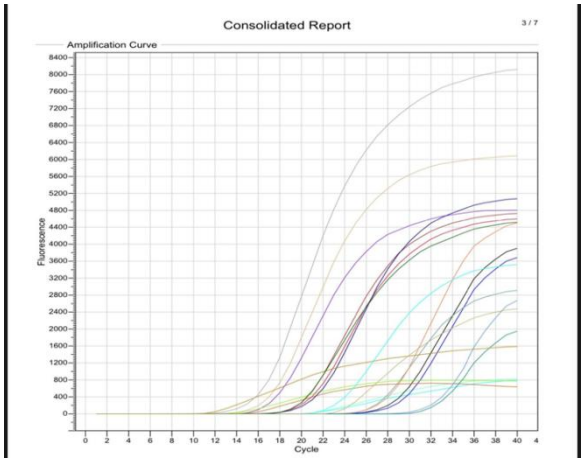

Fig. 8 *Real time PCR of copB and czcA genes*

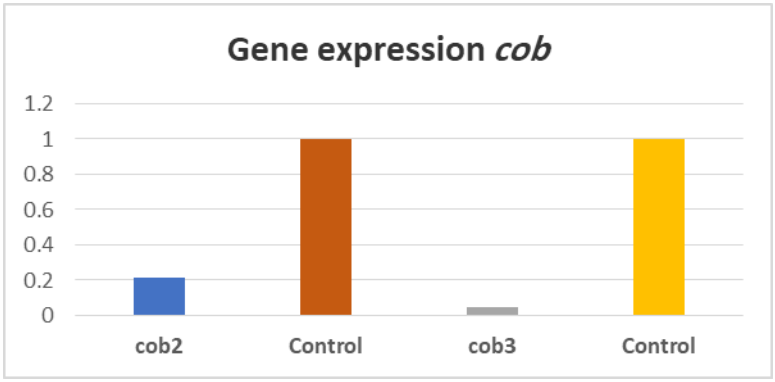

Fig. 9 *copB gene after treatment with CNPs*

Table 4: Gene expression of *copB Gene*

No.	Treatment	*Gene expression*	Folding	Conclusion
2	*copB2*	0.211	4.739336493	Down-regulation
	Control	1	1	Down-regulation
3	*copB3*	0.047	21.27659574	Down-regulation
	Control	1	1	Down-regulation

Fig. 10 *czcA gene after treating p.aeruginosa with CNPs*

Table 5: Gene expression *czc Gene*

No.	Treatment	*Gene expression*	Folding	Conclusion
10	*czcA10*	0.882	1.133786848	Down-regulation
	Control	1	1	Down-regulation
11	*czcA11*	0.392	2.551020408	Down-regulation
	Control	1	1	Down-regulation

These findings are consistent with a research on alkhalil, which explained AgNPs act selectively on cell wall receptors at specific sites, modifying the sporin protein channels and the permeability of P. aeruginosa's outer membrane. Finally, the examination of bacterial components according to supplement concentration indicates that the bacterial cells were significantly harmed by the action of AgNPs-CNTs [1].

A large surface area is made available for the attachment and dispersion when CNPs are present. Because of its larger surface area, the CNPs and bacteria can come into greater contact, which increases their antibacterial activity. Table 3 shows the effect of CNPs on the *copB gene* which is a putatively copper translocating ATPase. gene expression in sample3 was

(0.047) more effected by CNPs than sample 2; gene expression was (0.211), while the gene expression of the *czcA gene* in table 4 of sample 11 was more affected by CNPs (gene expression was 0.392) than sample 10 (gene expression was 0.882). These results are agreed with study of Khalil and et al [1].

The results showed that P. aeruginosa was especially susceptible to CNPs, as demonstrated by the antibacterial activity of CNPs against both bacteria, with minimal inhibitory levels of around 0.006 mg/l. Additionally, the expression variations of efflux pumps were investigated. CNP treatment significantly reduced the expression of the copB and czcA genes in both P. aeruginosa strains as compared to untreated samples, according to quantitative real-time PCR (qRT-PCR). These findings imply that CNPs cause oxidative and general stress, suppress the expression of virulence genes, and affect the integrity of cell membranes in P. aeruginosa. The impact of CNPs on the stress response and P. aeruginosa virulence and pathogenicity genes.

According to these findings, CNTs' method of action can be linked to their impact on P. aeruginosa's cell membrane integrity, suppression of virulence-gene expression, and generation of oxidative and general stress [1].

conclusion, Carbon nanoparticles obtained from walnut shells can be used as effective adsorbent materials to reduce gene expression in pathogenic bacteria.

References

[1] Khalil, A. M., Gharieb, M. A., Abdelaty, S. M., & El-Khatib, A. M. (2024). Antibacterial efficacy of decorated carbon nanotubes by nano silver against pseudomonas aeruginosa. *Materials Research Express*, *11*(7), 75006. DOI 10.1088/2053-1591/ad5f7d

[2[Shehan, M. A., Mahal, S. N., & Aljumaili, O. I. (2020). The Effect of Some Enzymes on the Formation of Biofilm from Bacterial Pseudomonas aeruginosa Isolated from Pathological Samples. *Systematic Reviews in Pharmacy*, *11*(2). DOI: 10.5530/srp.2020.2.67

[3] Novik, G., Savich, V., & Kiseleva, E. (2015). An insight into beneficial Pseudomonas bacteria. *Microbiology in Agriculture and Human Health*, *1*(5), 73–105.

[4] (kenooosh & shehan, 2022)Kenoosh, H. A., & Shehan, M. A. (2022). Relationship Quorum Sensing genes RhlR and Lasl to Production of Virulence Factors in Pseudomonas aeruginosa. *NeuroQuantology*, *20*(10), 5531. DOI: 10.14704/nq.2022.20.10.NQ55532

[5] Qin, M., Zhang, L., & Wu, H. (2022). Dielectric loss mechanism in electromagnetic wave absorbing materials. *Advanced Science*, *9*(10), 2105553. https://doi.org/10.1002/advs.202105553

[6] Xin, N., Guan, J., Zhou, C., Chen, X., Gu, C., Li, Y., Ratner, M. A., Nitzan, A., Stoddart, J. F., & Guo, X. (2019). Concepts in the design and engineering of single-molecule electronic devices. *Nature Reviews Physics*, *1*(3), 211–230.

[7] Moskvitina, E., Kuznetsov, V., Moseenkov, S., Serkova, A., & Zavorin, A. (2023). Antibacterial effect of carbon nanomaterials: Nanotubes, carbon nanofibers, nanodiamonds, and onion-like carbon. *Materials*, *16*(3), 957. https://doi.org/10.3390/ma16030957

[8] Ji, X., Peng, B., Ding, H., Cui, B., Nie, H., & Yan, Y. (2023). Purification, structure and biological activity of pumpkin polysaccharides: a review. *Food Reviews International*, *39*(1), 307–319. https://doi.org/10.1080/87559129.2021.1904973

[9] Khan, H., Yerramilli, A. S., D'Oliveira, A., Alford, T. L., Boffito, D. C., & Patience, G. S. (2020). Experimental methods in chemical engineering: X-ray diffraction spectroscopy—XRD. *The Canadian Journal of Chemical Engineering*, *98*(6), 1255–1266. https://doi.org/10.1002/cjce.23747
[10] Tang, C. Y., & Yang, Z. (2017). Transmission electron microscopy (TEM). In *Membrane characterization* (pp. 145–159). Elsevier.
[11] Mohammed, A., & Abdullah, A. (2018). Scanning electron microscopy (SEM): A review. *Proceedings of the 2018 International Conference on Hydraulics and Pneumatics—HERVEX, Băile Govora, Romania*, *2018*, 7–9. https://doi.org/10.1002/cjce.23747
[12] Alsaffar, H. M., Bertram, D., & Kalin, R. M. (2019). A comprehensive optimum integrated water resources management approach for multidisciplinary water resources management problems. *Journal of Environmental Management*, *239*, 211–224. https://doi.org/10.1016/j.jenvman.2019.03.045
[13] Green, M. R., & Sambrook, J. (2019). Analysis of DNA by agarose gel electrophoresis. *Cold Spring Harbor Protocols*, *2019*(1), pdb-top100388. doi:10.1101/pdb.top100388

[14] Muslim, H. B., & Al-Saadi, A. G. M. (2023). The Prevalence of some Heavy Metal Resistance Genes in Pseudomonas aeruginosa Isolated from Hospital Environments. *IOP Conference Series: Earth and Environmental Science*, *1262*(2), 22006. DOI 10.1088/1755-1315/1262/2/022006
[15] Fatimah, S., Ragadhita, R., Al Husaeni, D. F., & Nandiyanto, A. B. D. (2022). How to calculate crystallite size from x-ray diffraction (XRD) using Scherrer method. *ASEAN Journal of Science and Engineering*, *2*(1), 65–76. https://ejournal.kjpupi.id/index.php/ajse/article/view/283

[16] Gómez-Torres, M. J., Huerta-Retamal, N., Robles-Gómez, L., Sáez-Espinosa, P., Aizpurua, J., Avilés, M., & Romero, A. (2021). Arylsulfatase a remodeling during human sperm in vitro capacitation using field emission scanning electron microscopy (FE-SEM). *Cells*, *10*(2), 222. https://doi.org/10.3390/cells10020222

[17] Zuo, J. M., & Spence, J. C. H. (2017). *Advanced transmission electron microscopy*. Springer.
[18] Intorne, A. C., de Oliveira, M. V. V., de M Pereira] , L., & de Souza Filho, G. A. (2012). Essential role of the czc determinant for cadmium, cobalt and zinc resistance in Gluconacetobacter diazotrophicus PAl 5. *International Microbiology*, *15*(2), 69–78. https://doi.org/10.2436/20.1501.01.160. DOI: 10.2436/20.1501.01.160.

[19] Shartooh, S. M., Najeeb, L. M., & Sirhan, M. M. (2018). Biological treatment of carcinogenic acrylonitrile using Pseudomonas aeruginosa in Basra City. *J. Biol. Sci*, *18*, 415–424.

[20] Van der Zee, A., Kraak, W. B., Burggraaf, A., Goessens, W. H. F., Pirovano, W., Ossewaarde, J. M., & Tommassen, J. (2018). Spread of carbapenem resistance by transposition and conjugation among Pseudomonas aeruginosa. *Frontiers in Microbiology*, *9*, 2057.

IRAQI Academic Scientific Journals
Samarra Journal of Pure and Applied Science
SJPAS
مجلة سامراء للعلوم الصرفة والتطبيقية
www.sjpas.com
p ISSN: 2663-7405
e ISSN: 2789-6838

تأثير جزيئات الكربون النانوية في تقليل التعبير الجيني لجينات عوامل الضراوة في بكتريا الزائفه الزنجاريه

ساره عدنان خلف* سفيان محمد شرتوح، مياده عبد الله شيحان
قسم علوم الحياة، كلية العلوم، جامعة الانبار، الانبار، الرمادي، العراق.

معلومات البحث:
تاريخ الاستلام: 2025/01/11
تاريخ التعديل: 2025/02/15
تاريخ القبـــول: 2025/03/20
تاريخ الـنشر: 2025/12/30
الكلمات المفتاحية:
الزائفة الزنجارية، الامتصاص البيولوجي، الجسيمات النانوية الكربونية، المجهر الإلكتروني النافذ، المجهر الإلكتروني الماسح، حيود الأشعة السينية
معلومات المؤلف

الايميل:

الخلاصة:
لقد أصبح تلوث البيئة المائية بواسطة الزائفة الزنجارية تحديًا كبيرًا للبشر. يركز هذا البحث على دور جزيئات الكربون النانوية في تقليل انتشار البكتيريا وجينات عوامل ضراوتها. تم غسل قشور الجوز بالماء المقطر، وخلطها مع KOH، وحرقها عند درجة حرارة 650 درجة مئوية، ومعالجتها بالموجات فوق الصوتية للحصول على جزيئات الكربون النانوية. تم الحصول على العزلات البكتيرية من مواقع مختلفة من المياه في المستشفيات وكانت مميزة للزائفة. بعد ذلك تم إجراء (MIC) لتحديد التركيز الأمثل المؤثر على الزائفة الزنجارية وكان 0.006 ملغم/لتر، ثم تم استخدام التشخيص المظهري ثم الاختبارات البايوكيميائية لتشخيص بكتيريا p.aeruginosa وثم تفاعل البوليميراز المتسلسل (PCR) للكشف عن جينات عوامل الضراوة (copB و czcA). أثرت المساحة السطحية الكبيرة لجسيمات الكربون النانوية (CNPs) بتركيزات 0.006 جم / لتر بشكل كبير على نشاط CNPs على النقل الأفقي لجينات عامل الفوعة (CopB وczc). بعد العلاج، كان التعبير الجيني copB 0.211 للعزلة 2 و0.047 للعزلة 3، بينما كان التعبير الجيني 0.882 czcA للعزلة 10 و0.392 للعزلة 11. تم اختبار قدرة CNPs على تقليل التعبير الجيني في جينات عامل الفوعة باستخدام pcr الكمي (qpcr)، ونتيجة لذلك يؤثر على البكتيريا، فإن CNPs بتركيزات معينة لديها قدرة عالية على تحديد الفوعة. الجينات العوامل. تم دعم هذه النتائج من خلال فحص XRD (Panalytical 'X' Pert Pr، المملكة المتحدة)، والذي أشار إلى وجود ذروتي حيود Bragg في جسيمات الكربون النانوية، كما أشارت نتائج TEM (Zeiss LEO 912 AB/ ألمانيا) إلى وجود جسيمات غير متجانسة، وكذلك الشكل غير المنتظم لسطح جسيمات الكربون النانوية ذات المساحة السطحية الكبيرة حسب فحص SEM (Zeiss Sigma VP/ Germany